



Published in final edited form as:

*J Appl Physiol.* 2007 June ; 102(6): 2104–2111. doi:10.1152/jappphysiol.00033.2007.

## Myocardial Infarct Size Measurement in the Mouse Chronic Infarction Model: Comparison of Area- and Length-Based Approaches

Junya Takagawa<sup>1</sup>, Yan Zhang<sup>1</sup>, Maelene L. Wong<sup>1</sup>, Richard E. Sievers<sup>1</sup>, Neel K. Kapasi<sup>1</sup>, Yan Wang<sup>2</sup>, Yerem Yeghiazarians<sup>1</sup>, Randall J. Lee<sup>1</sup>, William Grossman<sup>1</sup>, and Matthew L. Springer<sup>1</sup>

<sup>1</sup>University of California, San Francisco, Department of Medicine, Division of Cardiology, San Francisco, California, U.S.A

<sup>2</sup>FivePrime Therapeutics, Inc., San Francisco, California, U.S.A

### Abstract

Efficacy of potential treatments for myocardial infarction (MI) is commonly assessed by histological measurement of infarct size in rodent models. In experiments involving an acute MI setting, measurement of the infarcted area in tissue sections of the left ventricle (LV) is a standard approach to determine infarct size. This approach has also been used in the chronic infarct setting to measure infarct area several weeks post-MI. We tested the hypothesis that due to wall thinning that is known to occur in the chronic setting, the area measurement approach would be less appropriate. We compared infarct measurements in tissue sections based on (1) infarct area, (2) epicardial and endocardial infarct arc lengths, and (3) midline infarct arc length. Infarct size from all three measurement approaches correlated significantly with LV ejection fraction (LVEF) and wall motion abnormality. However, the infarct size values derived from area measurement were significantly smaller than those from the other measurements, and the range of values obtained was compressed 0.4-fold. The midline method was able to detect the expected size differences between infarcts of variable severity resulting from proximal vs. distal ligation of the coronary artery. Segmental infarct size was correlated with segmental wall motion abnormality. We conclude that both area- and length-based measurements can determine relative infarct size over a wide range of severity but the area-based measurements are substantially more compressed due to wall thinning, and that the estimation of infarct midlines is a simple, reliable approach to infarct size assessment.

### Keywords

cardiac remodeling; area-based measurement; length-based measurement; histology

### Introduction

Rodent models of myocardial infarction (MI) have been employed frequently to elucidate the pathophysiological and molecular mechanisms of cardiac remodeling following the onset of MI (5,7,18,19,23,24). In recent years, the delivery of potentially therapeutic genes and the implantation of stem cells have attracted much interest and have been evaluated using rat or

Correspondence to: Matthew L. Springer, PhD Department of Medicine, Division of Cardiology University of California, San Francisco 513 Parnassus Avenue, Room S1136, Box 0124 San Francisco, CA 94143–0124 Tel: (415) 502–8404, Fax: (415) 502–8627 E-mail: E-mail: matt.springer@medicine.ucsf.edu.

mouse MI models (2,4,9,12,14,21,22). In many published studies exploring these potential therapies, success has commonly been evaluated by determination of infarct size, as well as functional and other histological parameters. In experiments involving an acute MI setting, infarct size is typically based on histological measurement of the area of the infarcted region in tissue sections of the left ventricle (LV) (13,16,20,26). In contrast, histological measurement of the arc length of the infarct scar has been commonly measured in a chronic MI setting (8, 14,18,19). Although it is well known that there is progressive thinning of the infarcted wall with reduction in the volume of the infarcted region (Figure 1) (6), area measurement is also used in the chronic infarct setting, taking infarct area measurements in tissue sections several weeks post-MI (9,10,23). In this study, we have compared histological infarct size derived from area- and length-based measurements in a chronic setting at 4 weeks after the onset of MI. Moreover, we have validated a simplified length-based measurement of infarct size, *midline length measurement*, that is comparable in sensitivity to the traditional length-based measurement approach.

## Materials and Methods

### Animals

Male C57BL/6 mice, aged 10 weeks, with body weight ranging from 22–28 g, were used for this study. All animal procedures were carried out in accordance with the guidelines of the Institutional Animal Care and Use Committee of the University of California, San Francisco.

### Induction of Myocardial Infarction

After anesthesia with isoflurane (4% induction, 2% maintenance), mice were intubated with polyethylene-50 tube (Intramedics, Becton-Dickinson; Sparks, MD) and connected to a small animal volume-control ventilator (Harvard Apparatus; Holliston, MA). Ventilation was done with a tidal volume of 350  $\mu$ l at 120 cycles/min. Each mouse was placed in a supine position on a heating table to prevent hypothermia during anesthesia. The heart was then exposed via a sternotomy with the use of a small retractor. The heart was positioned so that the LV, aorta and left atrium were exposed for suture placement. A 7-0 suture was placed in the anterior myocardium to occlude the left anterior descending artery (LAD). The heart was returned to its original position and a small piece of Sepra film (Genzyme Biosurgery, Cambridge, MA) was placed on the surface of the LV to reduce adhesions. The sternum incision was closed with 7-0 sutures and the skin incision was closed with 4-0 sutures. The endotracheal tube was gently retracted after spontaneous breathing was restored. Relatively large infarctions were induced by proximal ligation (4 mm from apex) of the LAD, and relatively small infarctions were induced by distal ligation (2 mm from the apex).

### Echocardiography

Transthoracic echocardiography was performed at 28 days after LAD ligation using a Vevo 660 system (VisualSonics, Toronto, Canada) equipped with a 30 MHz real time microvisualization scan head probe at a frame rate of 65 frames/sec. Each mouse was anesthetized with 1.5% isoflurane and placed on a heating table in a supine position, and its extremities were fixed to 4 electrocardiography leads on the table. The chest was shaved and further cleaned with a chemical hair remover (Nair) to minimize ultrasound attenuation. Warmed Aquasonic 100 gel (Parker Laboratories, Fairfield, NJ) was applied to the thorax surface to optimize visibility of the cardiac chambers. A parasternal long axis B-mode image was acquired with appropriate position of the probe so that the maximum LV length could be identified. Three short axis B-mode images of the LV were taken at basal, mid-ventricular, and apical levels of the LV. Using the frames of the long axis image with the maximal and minimal cross sectional area in a heart cycle, LV end-systolic and end-diastolic volume (LVESV, LVEDV) were calculated respectively with the following formula: LV volume =  $(8 / 3\pi) \times$

(endocardial area<sup>2</sup> / endocardial long axis length) (25). Average LV volumes were calculated from three representative measurements over multiple heart cycles. LV ejection fraction (LVEF) was calculated as  $LVEF = [(LVEDV - LVESV) / LVEDV] \times 100$ . Three short axis images were used to obtain wall motion score index (WMSI) (25). The myocardium at basal and mid-ventricular levels was divided into 6 segments, and at the apical level into 4 segments. Regional wall motion in each segment was scored as 1-normal, 2-hypokinetic, 3-akinetic, 4-dyskinetic and 5-aneurysmal. WMSI was defined as the total of the wall motion scores divided by the number of segments scored. LVEF and WMSI were used to validate infarct sizes derived from three measurement approaches.

### Preparation of Heart Sections

After echocardiography, the heart was excised under deep anesthesia with inhalation of 5% isoflurane. In some cases described below, 0.1 ml saturated KCl was injected into the LV chamber before the hearts were harvested to arrest them in diastole (1,3,4,10). The left and right atria and large vessels were resected, the heart was washed with saline, embedded in O.C.T. compound (Sakura Finetechnical USA, Inc., Torrance, CA), and frozen in a bath of 2-methylbutane with dry ice. The hearts were stored at  $-80^{\circ}\text{C}$  and sliced transversely from the apex to the basal part of the LV with the use of a cryostat at 6  $\mu\text{m}$  thickness with the interval of 300  $\mu\text{m}$  between each section. All sections were mounted on glass slides and stained with Masson trichrome stain for quantitative analysis of infarct size.

### Measurement of infarct size

All histological sections were examined with a Nikon Eclipse E800 microscope using a 1x objective. Images were captured with a Retiga CCD camera with the use of Openlab software (Improvision, Lexington, MA). ImageJ 1.34 software was used to measure lengths and areas of infarct and LV. The scar was measured in each section by an investigator who was blinded to the identity of the sections using the following three approaches:

**1) Area measurement**—Infarct scar area and the total area of LV myocardium were traced manually in the digital images and measured automatically by the computer. Infarct size, expressed as a percentage, was calculated by dividing the sum of infarct areas from all sections by the sum of LV areas from all sections (including those without infarct scar) and multiplying by 100.

**2) Length measurement**—Four lengths, including epicardial and endocardial infarct lengths, and epicardial and endocardial circumferences, were traced manually in the digital images and measured automatically by the computer. To define the infarct lengths, endocardial infarct length was taken as the length of endocardial infarct scar surface that included greater than 50% of the whole thickness of myocardium, and epicardial infarct length as the length of the transmural infarct region (Figure 2). Epicardial infarct ratio was obtained by dividing the sum of epicardial infarct lengths from all sections by the sum of epicardial circumferences from all sections. Endocardial infarct ratio was calculated similarly. Infarct size derived from this approach was calculated as  $[(\text{epicardial infarct ratio} + \text{endocardial infarct ratio}) / 2] \times 100$ .

**3) Midline length measurement**—The LV myocardial midline was drawn at the center between the epicardial and endocardial surfaces and the length of the midline was measured as midline circumference. Midline infarct length was taken as the midline of the length of infarct that included greater than 50% of the whole thickness of the myocardial wall. Infarct size derived from midline length measurement was calculated by dividing the sum of midline infarct lengths from all sections by the sum of midline circumferences from all sections and multiplying by 100.

Segmental histological infarct size was also measured using area and midline length measurement. A section at mid-ventricular level was selected and the LV wall was divided into 6 segments, similar to the assessment of echocardiographic wall motion abnormality. The area and the midline length of each segment, and of the infarct region in each segment, were measured in similar fashion to each measurement approach described above. The segmental infarct size was calculated as the percentage of infarct area or length in each segment.

### Statistical Analysis

All data are expressed as mean  $\pm$  SD. Analysis of variance was used for comparison of more than two groups. Unpaired t-test was applied to the comparison between two groups. Correlations between infarct size and LVEF and between infarct size and WMSI were tested by linear regression analysis.  $P < 0.05$  was considered statistically significant.

## Results

### Validation of three measurement approaches for infarct size assessment

MI was induced in 23 mice, and both LVEF and WMSI were measured by echocardiography at 28 days post-MI, after which the hearts were harvested, sectioned, and stained with Masson trichrome to visualize the infarct scar. We then calculated infarct size scores using the three measurement approaches for infarct size, described in the Methods section: (1) an area measurement approach, (2) a length measurement approach based on epicardial and endocardial scar arc lengths, and (3) a simplified midline length measurement approach. Figure 3 shows the range of values obtained with each approach. The order of the values was mostly consistent from method to method. However, the infarct size values obtained using area measurement were significantly smaller than those using length measurement and midline length measurement (area measurement  $12.0 \pm 5.9\%$  vs. length measurement  $30.1 \pm 15.5\%$ , midline length measurement  $29.9 \pm 16.5\%$ ,  $p < 0.01$ ), and the range of values obtained was compressed 0.4-fold. Linear regression analyses showed that infarct size values from all three measurement approaches correlated significantly with both LVEF and WMSI (Figure 4). The segmental infarct size was measured on a histological section at mid-ventricular level in 8 of these hearts. The segmental infarct size derived from both the area and midline length measurement approaches also significantly increased with the severity of wall motion abnormality in that segment (Figure 5). These results indicate that area measurement can be used to represent the relative sizes of a group of infarct scars at 28 days after LAD ligation, but that the resulting values are compressed compared to those obtained by both length-based measurement approaches.

### Minimum number of sections per heart required for reliable measurement of infarct size

To assess the minimum number of sections per heart required for the reliable measurement of infarct size, we calculated infarct sizes for each heart in the previous experiment using progressively smaller subsets of sections. As detailed in Figure 6, infarct sizes from each heart were calculated using all, one-half (1/2), one-third (1/3), one-fourth (1/4), and one-fifth (1/5) of the sections initially collected. ("All" refers to sections collected at 300  $\mu$ m intervals, see Methods.) The average number of sections counted for each condition was  $19.3 \pm 2.4$  for "all" sections,  $9.9 \pm 1.1$  in 1/2 sections,  $6.7 \pm 0.9$  in 1/3 sections,  $5.2 \pm 0.6$  in 1/4 sections, and  $3.7 \pm 0.5$  in 1/5 sections. Infarct size values for each heart remained consistent for all, 1/2, and 1/3 subsets, especially using both length-based approaches, and variability was substantially greater starting with the 1/4 subset based on comparisons within each animal (Figure 6). To quantify this variability for each subset of sections, we calculated the absolute value of the deviation from the infarct size derived from all sections. The reduction of the number of sections measured caused a significant increase in the deviation of infarct size obtained (Figure 7). The correlation coefficients between infarct size and both LVEF and WMSI were high using

all subsets of sections. We conclude that while reasonable values can be calculated using 1/4 or 1/5 of the sections, use of 1/3 of the sections is optimal and there is little to be gained from including more sections than 1/3 in the analysis.

### The further validation of midline length measurement

Because the previous analyses were performed retrospectively in a range of infarcts from a single group, we performed a prospective study in which infarcts of different expected sizes were induced by ligation of the LAD in 2 different locations. MI was induced by proximal ligation (4 mm from apex) and distal ligation (2 mm from apex) of the LAD in 8 mice per group. All mice underwent echocardiography at 4 weeks post-MI. The infarct size was determined using midline length measurement. Because one mouse that underwent proximal ligation died during observation period, infarct size was measured in a total of 15 infarcted hearts (proximal ligation; n=7, distal ligation; n=8). Midline length measurement successfully distinguished between predicted large and small infarcts induced by different ligation sites (proximal ligation  $33.6 \pm 8.53\%$  vs. distal ligation  $13.8 \pm 5.3\%$ ,  $p < 0.01$ ). The significant correlation between infarct size and LVEF was also observed in this experiment (n=15,  $r = 0.87$ ,  $p < 0.01$ ).

### Discussion

In this study we have demonstrated that infarct size values measured by area-based and length-based approaches at 28 days post-MI were highly correlated with cardiac systolic dysfunction, but that infarct size values obtained with area measurement were significantly compressed compared to those using the length-based approaches.

Cardiac remodeling following the onset of MI is accompanied by structural changes in the LV, such as chamber dilatation, wall thinning in the infarcted region, and hypertrophy in the viable region (11,17,18). These changes imply that the opposing changes of wall thickness in dead and viable myocardium may obscure the relationship between the functional severity of MI and the resulting percentage of infarct scar volume, which is the parameter measured by area-based approaches. In contrast, length-based approaches measure the extent to which the infarct scar radially covers the wall of the left ventricle, without being influenced by thinning of the wall.

Fishbein et al. (6) conducted early studies using a rat model of MI in which they quantified histological infarct size, and determined that there was progressive thinning of the infarcted wall with reduction in volume of the MI throughout its evolution, but no decrease in the percentage of the surface area of the LV involved. In a mouse model of MI, Virag et al. (23) showed that infarct size using area-based measurement reduced from  $38 \pm 5\%$  at 4 days to  $20 \pm 4\%$  at 28 days after LAD ligation with the formation of scar tissue, and Lutgens et al. (11) found that infarct size measured by a length-based measurement was similar from 1 week through 5 weeks after the onset of MI despite a progressive increase in LV diameter. Although these reports support and supplement our results, infarct sizes in these studies were not validated by comparison to the severity of cardiac dysfunction. Kanno et al. (8) estimated infarct size by obtaining infarct areas from sequential B-mode echocardiographic short axis images in a mouse MI model and demonstrated significant correlations between the estimated infarct size, the histological infarct size using area-based measurement, and LVEF. However, they assessed infarct size only in the acute setting, at 1 day and 1 week after LAD ligation, during which the structural changes of the LV due to cardiac remodeling are still in progress. Although Gao et al. (7) reported significant relationships between infarct size and fractional shortening measured by echocardiography at 9 weeks after the onset of MI, they used only length-based measurement. In the present study, we directly compared infarct size values obtained using area- and length-based measurement approaches in a chronic MI setting, and

determined that infarct sizes derived from area measurement, length measurement and midline length measurement all reflect the severity of systolic dysfunction. However, we observed that infarct size scores obtained from the area measurement were substantially lower compared with those using length measurement and midline length measurement. Our results indicates that area- and length-based measurement approaches are both reasonable, but length-based approaches are able to document changes in the severity of the infarction with greater resolution than area-based measurement in a chronic MI setting.

The advantage of the midline length measurement that we have proposed in this study over the commonly-used epicardial/endocardial measurement approach is that the number of measurements required for each tissue section is reduced 2-fold, substantially increasing time-efficiency. Despite reducing the number of measurements per section, infarct size values derived from midline length measurement were almost identical to those using length measurement in 23 infarcted mouse hearts with a wide range of cardiac systolic dysfunction. Moreover, midline length measurement successfully distinguished between large infarcts and small infarcts induced by different LAD ligation sites. Therefore, we propose that midline length measurement for assessment of infarct size is a relatively simple yet reliable alternative to those approaches currently in common use.

An alternative strategy for the assessment of chronic infarct size is to estimate the amount of missing myocardium (15). Because it is based on the extent of myocardial death, rather than the remaining scar, this concept is quite sensible and is likely to yield the measurements that best reflect the severity of an infarct in the ideal situation. However, it is difficult to obtain a reliable measure of the missing myocardium without making assumptions based on the relationships between mass, cell number, and wall thickness in average hearts, which can be of uncertain validity for the specific hearts in a given experiment. Potentially for this reason, most investigators have opted to base their histological assessments of chronic infarct size on either area- or arc length-based measurement approaches. While none of these histological measurements or even functional measurements serve as a gold standard for infarct severity, they strengthen each other by being able to rank a series of infarcts in a relatively consistent order. Similarly, a limitation of the functional measurement aspect of this study is that the echocardiographic frame rate is relatively low compared to the high beat rate of the mouse heart (~8 frames/heart cycle). However, our measurements taken over three heart cycles were consistent with the corresponding histological measurements. Therefore, while none of the approaches discussed here result in perfect representations of the consequences of MI, we propose that the midline length measurement presents a simple approach that makes minimal assumptions, and does not sacrifice sensitivity relative to the more commonly-used epicardial/endocardial length approach.

In spite of the widespread uses of histological infarct size measurement in mouse MI models, the studies of which we are aware have not explored the minimum number of sections to be measured for the reliable calculation of infarct size. The most accurate infarct size determination theoretically derives from the use of 100% of the tissue, but the standard approach is to cut tissue sections at defined intervals and to discard the rest of the tissue. Even for the tissue sections that are collected, we hypothesized that progressively smaller subsets of sections could be measured with insignificant loss of accuracy, until a certain point at which the number of sections is too small and the resulting numbers begin to deviate from the theoretical “real” number. To address this issue, we calculated the deviation of infarct size measurements derived from different numbers of sections per heart from those using all sections. Our results showed that there was a significant increase or a tendency to increase in the deviation of infarct size between 1/5 (3–4 sections per heart) and 1/2 (9–11 sections per heart) of all sections. Although infarct size using 1/5 and 1/4 of all sections still correlates with

the severity of cardiac dysfunction, that the point at which both simplicity and reliability are maximized appears to be measurement of 6–8 sections (1/3 of all sections).

We conclude that (1) both area- and length-based measurements can determine relative infarct size over a wide range of severity but the area-based measurements are substantially more compressed; (2) midline length measurement is a reliable and simple way to assess infarct size compared to conventional length measurement approaches; and (3) measurement of 6–8 tissue sections per heart is optimal for the assessment of infarct size using length based methods. We propose that this approach to assessment of chronic infarct size is well suited for experiments involving potential therapies for MI when assessed in a chronic setting.

## Acknowledgements

We wish to thank Ngan Huang for helpful discussions.

### Grants

This research was supported by a grant from the Wayne and Gladys Valley Foundation to W.G., and by grants from the National Institutes of Health (National Institute of Biomedical Imaging and Bioengineering 1 R03 EB005802), the American Heart Association, the UC Industry-University Cooperative Research Program, and FivePrime Therapeutics to M.L.S.

## References

1. Ahn D, Cheng L, Moon C, Spurgeon H, Lakatta EG, Talan MI. Induction of myocardial infarcts of a predictable size and location by branch pattern probability-assisted coronary ligation in C57BL/6 mice. *Am J Physiol Heart Circ Physiol* 2004;286:H1201–1207. [PubMed: 14766681]
2. Christman KL, Fang Q, Yee MS, Johnson KR, Sievers RE, Lee RJ. Enhanced neovasculature formation in ischemic myocardium following delivery of pleiotrophin plasmid in a biopolymer. *Biomaterials* 2005;26:1139–1144. [PubMed: 15451633]
3. Curcio A, Noma T, Naga Prasad SV, Wolf MJ, Lemaire A, Perrino C, Mao L, Rockman HA. Competitive displacement of phosphoinositide 3-kinase from beta-adrenergic receptor kinase-1 improves postinfarction adverse myocardial remodeling. *Am J Physiol Heart Circ Physiol* 2006;291:H1754–1760. [PubMed: 16699071]
4. Dai W, Hale SL, Martin BJ, Kuang JQ, Dow JS, Wold LE, Kloner RA. Allogeneic mesenchymal stem cell transplantation in postinfarcted rat myocardium: short- and long-term effects. *Circulation* 2005;112:214–223. [PubMed: 15998673]
5. Engberding N, Spiekermann S, Schaefer A, Heineke A, Wiencke A, Muller M, Fuchs M, Hilfiker-Kleiner D, Hornig B, Drexler H, Landmesser U. Allopurinol attenuates left ventricular remodeling and dysfunction after experimental myocardial infarction: a new action for an old drug? *Circulation* 2004;110:2175–2179. [PubMed: 15466649]
6. Fishbein MC, Maclean D, Maroko PR. Experimental myocardial infarction in the rat: qualitative and quantitative changes during pathologic evolution. *Am J Pathol* 1978;90:57–70. [PubMed: 619696]
7. Gao XM, Dart AM, Dewar E, Jennings G, Du XJ. Serial echocardiographic assessment of left ventricular dimensions and function after myocardial infarction in mice. *Cardiovasc Res* 2000;45:330–338. [PubMed: 10728353]
8. Kanno S, Lerner DL, Schuessler RB, Betsuyaku T, Yamada KA, Saffitz JE, Kovacs A. Echocardiographic evaluation of ventricular remodeling in a mouse model of myocardial infarction. *J Am Soc Echocardiogr* 2002;15:601–609. [PubMed: 12050601]
9. Kudo M, Wang Y, Wani MA, Xu M, Ayub A, Ashraf M. Implantation of bone marrow stem cells reduces the infarction and fibrosis in ischemic mouse heart. *J Mol Cell Cardiol* 2003;35:1113–1119. [PubMed: 12967634]
10. Lal A, Veinot JP, Ganten D, Leenen FH. Prevention of cardiac remodeling after myocardial infarction in transgenic rats deficient in brain angiotensinogen. *J Mol Cell Cardiol* 2005;39:521–529. [PubMed: 15950985]

11. Lutgens E, Daemen MJ, de Muinck ED, Debets J, Leenders P, Smits JF. Chronic myocardial infarction in the mouse: cardiac structural and functional changes. *Cardiovasc Res* 1999;41:586–593. [PubMed: 10435030]
12. Mangi AA, Noiseux N, Kong D, He H, Rezvani M, Ingwall JS, Dzau VJ. Mesenchymal stem cells modified with Akt prevent remodeling and restore performance of infarcted hearts. *Nat Med* 2003;9:1195–1201. [PubMed: 12910262]
13. Michael LH, Ballantyne CM, Zachariah JP, Gould KE, Pocius JS, Taffet GE, Hartley CJ, Pham TT, Daniel SL, Funk E, Entman ML. Myocardial infarction and remodeling in mice: effect of reperfusion. *Am J Physiol* 1999;277:H660–668. [PubMed: 10444492]
14. Orlic D, Kajstura J, Chimenti S, Jakoniuk I, Anderson SM, Li B, Pickel J, McKay R, Nadal-Ginard B, Bodine DM, Leri A, Anversa P. Bone marrow cells regenerate infarcted myocardium. *Nature* 2001;410:701–705. [PubMed: 11287958]
15. Orlic D, Kajstura J, Chimenti S, Limana F, Jakoniuk I, Quaini F, Nadal-Ginard B, Bodine DM, Leri A, Anversa P. Mobilized bone marrow cells repair the infarcted heart, improving function and survival. *Proc Natl Acad Sci U S A* 2001;98:10344–10349. [PubMed: 11504914]
16. Park SW, Lee SY, Park SJ, Lee SC, Gwon HC, Kim DK. Quantitative assessment of infarct size in vivo by myocardial contrast echocardiography in a murine acute myocardial infarction model. *Int J Cardiol* 2004;97:393–398. [PubMed: 15561324]
17. Patten RD, Aronovitz MJ, Deras-Mejia L, Pandian NG, Hanak GG, Smith JJ, Mendelsohn ME, Konstam MA. Ventricular remodeling in a mouse model of myocardial infarction. *Am J Physiol* 1998;274:H1812–1820. [PubMed: 9612394]
18. Pfeffer JM, Pfeffer MA, Fletcher PJ, Braunwald E. Progressive ventricular remodeling in rat with myocardial infarction. *Am J Physiol* 1991;260:H1406–1414. [PubMed: 2035662]
19. Pfeffer MA, Pfeffer JM, Fishbein MC, Fletcher PJ, Spadaro J, Kloner RA, Braunwald E. Myocardial infarct size and ventricular function in rats. *Circ Res* 1979;44:503–512. [PubMed: 428047]
20. Piot CA, Padmanaban D, Ursell PC, Sievers RE, Wolfe CL. Ischemic preconditioning decreases apoptosis in rat hearts in vivo. *Circulation* 1997;96:1598–1604. [PubMed: 9315553]
21. Springer ML, Sievers RE, Viswanathan MN, Yee MS, Foster E, Grossman W, Yeghiazarians Y. Closed-chest cell injections into mouse myocardium guided by high-resolution echocardiography. *Am J Physiol Heart Circ Physiol* 2005;289:H1307–1314. [PubMed: 15908468]
22. Su H, Joho S, Huang Y, Barcena A, Arakawa-Hoyt J, Grossman W, Kan YW. Adeno-associated viral vector delivers cardiac-specific and hypoxia-inducible VEGF expression in ischemic mouse hearts. *Proc Natl Acad Sci U S A* 2004;101:16280–16285. [PubMed: 15534198]
23. Virag JI, Murry CE. Myofibroblast and endothelial cell proliferation during murine myocardial infarct repair. *Am J Pathol* 2003;163:2433–2440. [PubMed: 14633615]
24. Yamaguchi O, Higuchi Y, Hirotsu S, Kashiwase K, Nakayama H, Hikoso S, Takeda T, Watanabe T, Asahi M, Taniike M, Matsumura Y, Tsujimoto I, Hongo K, Kusakari Y, Kurihara S, Nishida K, Ichijo H, Hori M, Otsu K. Targeted deletion of apoptosis signal-regulating kinase 1 attenuates left ventricular remodeling. *Proc Natl Acad Sci U S A* 2003;100:15883–15888. [PubMed: 14665690]
25. Zhang Y, Takagawa J, Sievers R, Khan MF, Viswanathan M, Springer ML, Foster E, Yeghiazarians Y. Validation of the Wall Motion Score and Myocardial Performance Indices As Novel Techniques to Assess Cardiac Function in Mice Post Myocardial Infarction. *Am J Physiol Heart Circ Physiol* 2007;292:H1187–1192. [PubMed: 17028161]
26. Zhu B, Sun Y, Sievers RE, Browne AE, Pulkurthy S, Sudhir K, Lee RJ, Chou TM, Chatterjee K, Parmley WW. Comparative effects of pretreatment with captopril and losartan on cardiovascular protection in a rat model of ischemia-reperfusion. *J Am Coll Cardiol* 2000;35:787–795. [PubMed: 10716484]



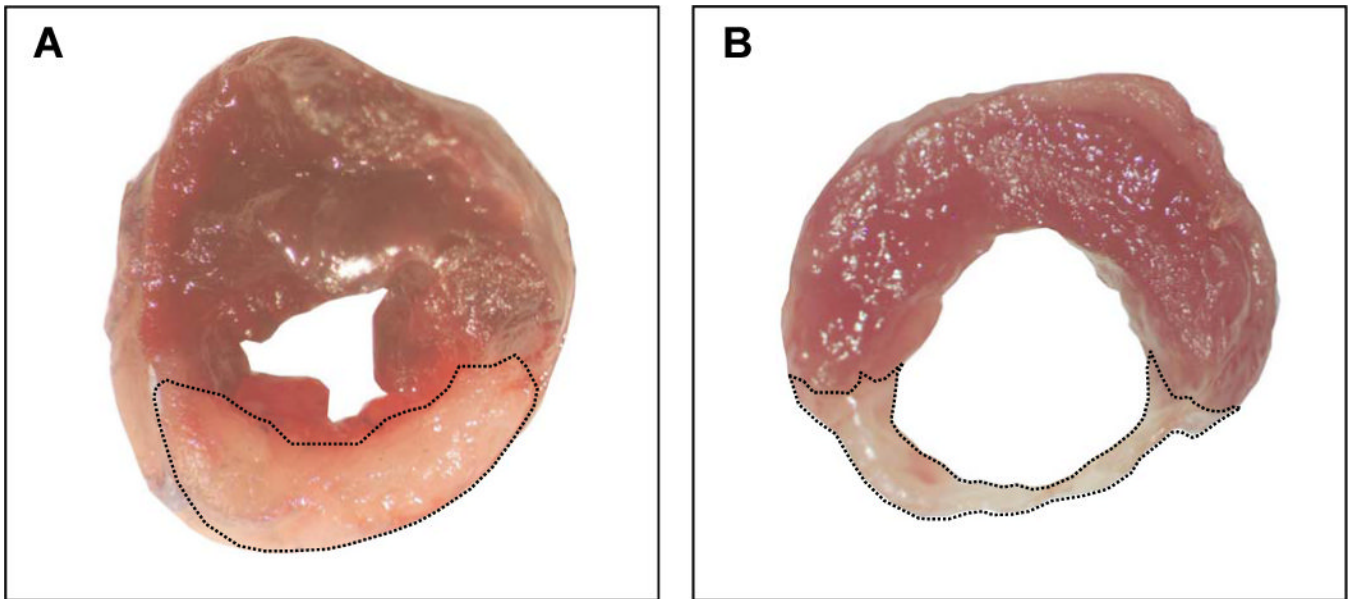


**Figure 1.** Comparison of infarct area in transversely sectioned hearts excised at (A) 1 day and (B) 28 days after the onset of myocardial infarction. The area surrounded by a broken line indicates infarct area.

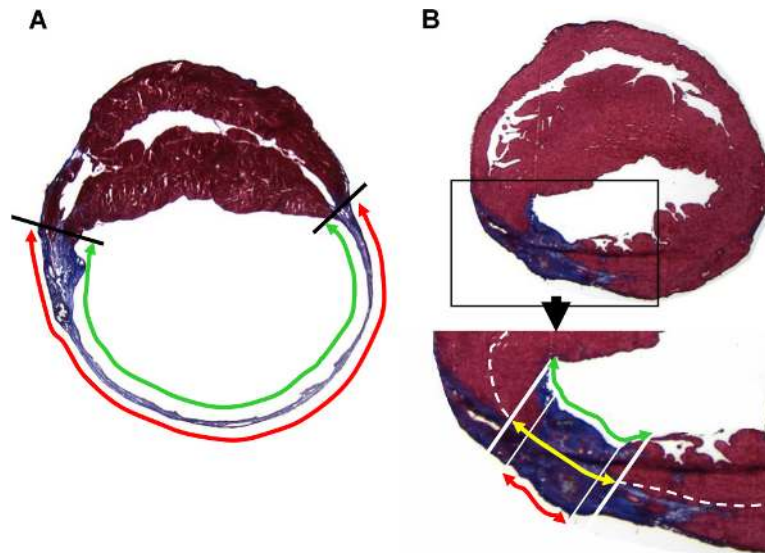


**Figure 2.**

The infarct region of section (A) consists only of scar tissue, but that of section (B) includes scar and viable tissue. To define the infarct lengths for the measurement of the latter case, endocardial infarct length (green arrow) was taken as the length of infarct that includes more than 50% of the whole thickness of myocardium, and epicardial length (red arrow) as the length of transmural infarct region. The broken white line marks the midline of the myocardium and the yellow arrow marks the midline length of the infarct scar. The thin solid white lines mark the extent of the transmural infarct, and the thick solid white lines mark the extent of the infarct that includes greater than 50% of the whole thickness of the myocardium. All measurements were blinded.

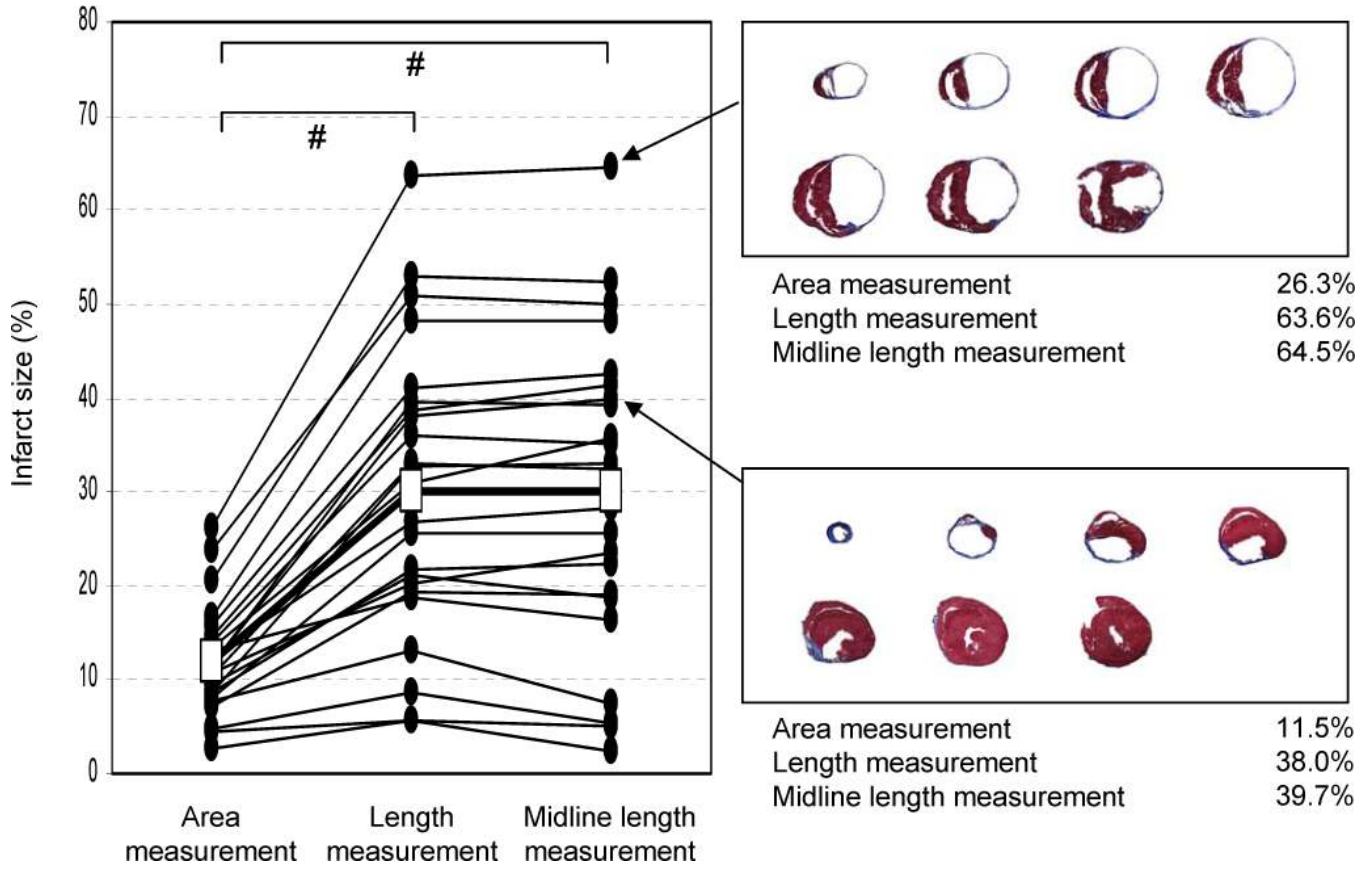


**Figure 3.** Infarct size obtained from the three measurement approaches. The infarct size using area measurement was significantly smaller than those using the length-based measurements. The difference between area measurement and both length measurement methods became larger with increasing infarct size. Mean values are denoted by open squares. #;  $p < 0.01$ .

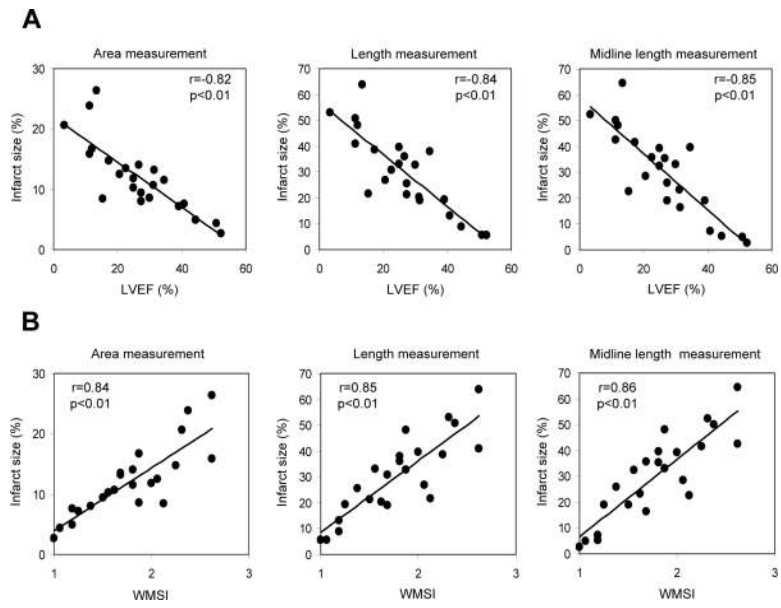


**Figure 4.** Linear correlations between infarct size derived from the three measurement approaches and: (A) left ventricular ejection fraction (LVEF), and (B) wall motion score index (WMSI) measured by echocardiography.

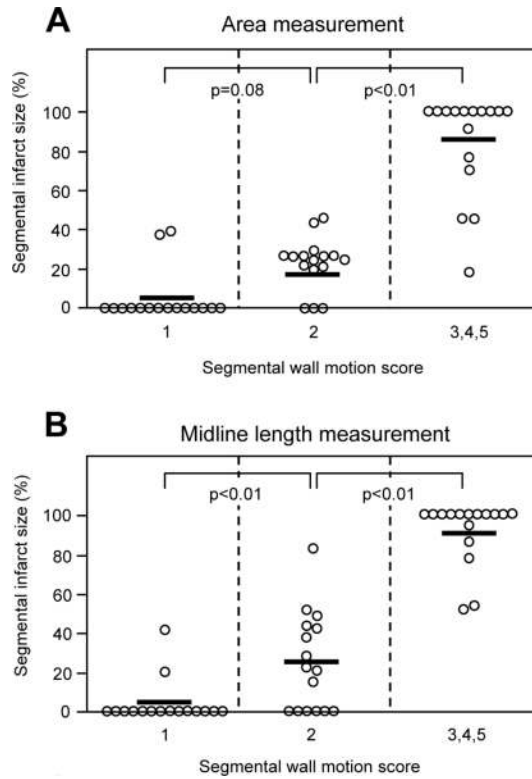


**Figure 5.**

The relation between the segmental histological infarct size and the echocardiographic wall motion score (1=normokinesis, 2=hypokinesis, 3=akinesis, 4=dyskinesis, 5=aneurysm) in the corresponding segment at midventricular level. No distinction is made here between scores of 3, 4, and 5 because their difference applies to global wall motion, rather than motion of individual wall segments. (A) infarct size derived from area measurement, (B) infarct size derived from midline length measurement. The bold line indicates the mean value of each subgroup.

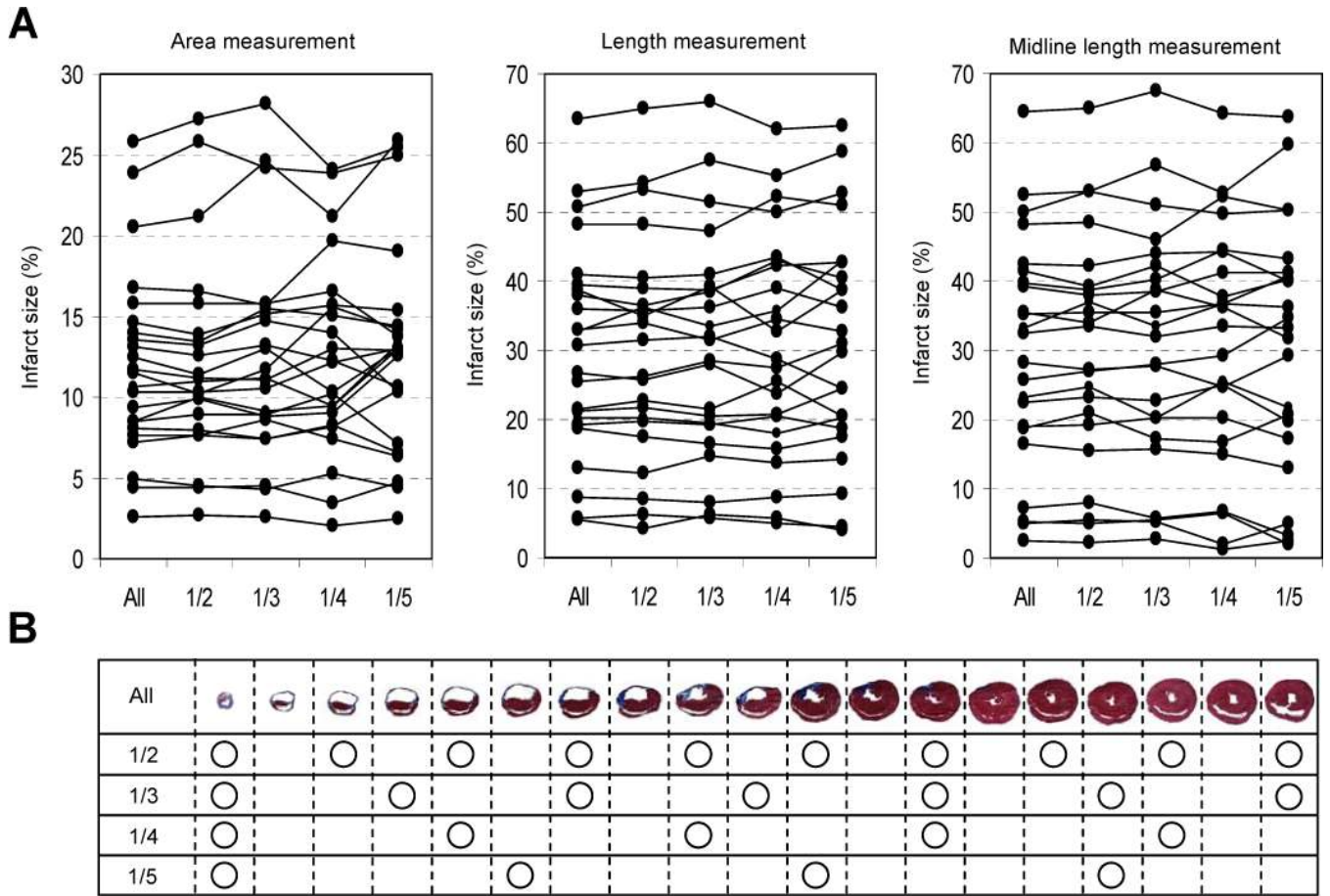


**Figure 6.** (A) Infarct size obtained from the three measurement approaches using different numbers of sections in 23 infarcted hearts. (B) An example of histological sections taken from an infarcted heart. The sections were taken from the apex through the basal part of the left ventricle at regular intervals according to the number of sections measured in each group. Circles indicate the sections selected in each subset for the measurement of infarct size.

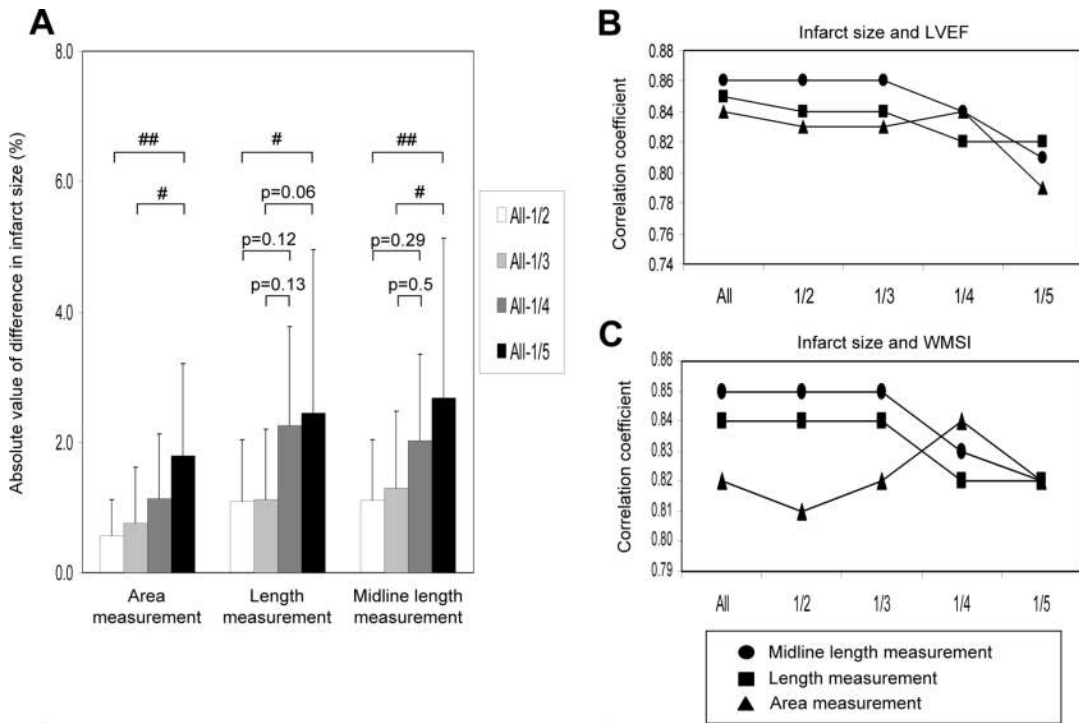


**Figure 7.** (A) The average deviation of infarct size obtained from different subsets of sections from that obtained from all sections. This represents the variability encountered by measuring scars in different numbers of sections. #;  $p < 0.05$ , ##;  $p < 0.01$ . (B) Correlation coefficients between left ventricular ejection fraction (LVEF) and infarct size values derived from the 3 measurement methods using 5 different numbers of sections. (C) Correlation coefficients between wall motion score index (WMSI) and infarct size values derived from the different approaches.